Defence Science Journal, Vol. 72, No. 4, July 2022, pp. 543-557, DOI : 10.14429/dsj.72.17329


# Ballistic Studies of the Rotational Motion of the Artillery Projectile into Account the Equatorial Damping Moment

Oleksandr M. Shyiko,* and Olexii A. Obukhov

*National Agricultural University, Sumy, Ukraine*
**E-mail:oleksandr.shyiko@yahoo.com*

**ABSTRACT**

The problem of calculating the equatorial damping moment during trajectory flight is an actual problem in ballistic studies of the rotational motion of artillery projectiles. The practice of ballistic research needs short algorithms that make it possible to calculate the damping moment together with the calculations of the trajectory parameters under conditions of continuously changing characteristics of the oncoming flow. In this regard, a simplified method for calculating the equatorial damping moment of artillery projectiles in the oncoming flow is proposed, based on the differentiation of the dependence for the overturning aerodynamic moment by the angle of attack and the Mach number of the oncoming flow. Calculations of the parameters of the rotational motion of the 155-mm artillery projectile on the flight trajectory have been carried out. The influence of the equatorial damping moment on the periodic components of the angular displacements of the projectile is revealed. The results of ballistic calculations with the loss of stability of the rotational motion of the projectile showed the destabilizing effect of the equatorial damping moment on the boundary parameters in terms of stability in the case of opposite directions of rotation of the projectile and crosswind.

**Keywords:** Artillery projectile; Ballistic studies; Flight trajectory; Angular displacements; Equatorial damping moment; Loss of stability

## 1. INTRODUCTION

The task of ensuring the stability of the movement of rotating artillery projectiles remains of particular relevance due to the constant striving to increase the firing range and power of rifled artillery charges. Numerous scientific works are devoted to the theoretical study of the disturbed rotational motion of a gyroscopically stabilized rotation bodies of the artillery projectile type, for example[1-5]. The results of these works contain linearized differential equations describing the perturbed precessional rotational motion of the projectile in the presence of the spatial angle of attack. For these systems of differential equations, analytical solutions are found[1-5], which determine the frequencies and amplitudes of the components of the precessional motion.

A significant number of works are devoted to the computational analysis of the precessional rotational motion of the projectile on the flight trajectory.[6,7,8] For example, the paper[6] presents results of numerical research on the effect of the twist rate, muzzle velocity, cross and longitudinal wind on the stability of flight of the 155- mm artillery projectile for flat and steep trajectories. The computational analysis of the component spatial angle of attack in pitch and yaw throughout the computational trajectory of the projectile is presented in reference.[8] Classical works on the study of the angular motion of fast rotating projectiles using the theory of stability of Lyapunov, it was established that with a full system of forces acting on the artillery projectile, the motion corresponding to the ideally correct flight is asymptotically unstable according to Lyapunov[4]. The motion, unstable according to Lyapunov, on a limited time interval can satisfy the criterion of technical stability[4]. Analysis of the solutions of the systems of differential equations of the perturbed precessional rotational motion of the projectile made it possible to establish a number of similar criteria for the gyroscopic stability of the projectile[1,2,4,6,8], the fulfillment of which ensures the stability of motion over a finite time interval of flight along the trajectory. The existence of modern computer technologies for numerical simulation changes the approach to solving many applied problems of aerodynamics and external ballistics. In this regard, it is important to use the results of modeling the aerodynamic characteristics of supersonic rotation bodies for the purposes of ballistic design.

A review of works devoted to the ballistic study of the rotational motion of artillery projectile indicates that one of the topical problems is the problem of calculating the equatorial damping moment on the calculated flight trajectory. The solution to this problem is seen in the development of methods for calculating the equatorial damping moment, which make it possible to implement them together with algorithms for calculating the parameters of the trajectory under conditions of continuously changing characteristics of the oncoming flow.

The purpose of this work is to develop a simplified method for calculating the equatorial damping moment of

Received : 15 July 2021, Revised : 5 April 2022
Accepted : 5 July 2022, Online published : 26 August 2022

an axisymmetric rotation body in the counterflow and the ballistic study of the perturbed rotational motion of the artillery projectile, taking into account the equatorial damping moment. The proposed calculation method is based on the differentiation of the dependence for the overturning aerodynamic moment by the angle of attack and the Mach number of the oncoming flow. In this case, a differentiable dependence can be obtained both by numerical simulation and on the basis of existing computational and experimental techniques or special experiments. The purpose of the computational ballistic research is to study the influence of the equatorial damping moment on the magnitude of the periodic and non-periodic components of the angular displacements and on the stability-limiting parameters of the rotational precessional motion of the projectile under the action of various destabilizing factors.

## 2. METHODOLOGY

In this work, for the computational study of the perturbed rotational motion of a gyroscopically stabilized dynamically balanced artillery projectile relative to its center of mass, we use equations obtained from the equations of the spatial motion of an artillery projectile in the form of V. S. Pugachev[4]. To write these equations, the starting system of axes $OXYZ$ (not shown), the trajectory system of axes $CTNB$ and the semi-connected system of axes $C\zeta\xi\eta$ (moves with the body, but does not participate in its rotation) are used (Fig. 1(a)). In Fig. 1(a,b) shows an attached starting coordinate system $OX'Y'Z'$ that is parallel to the starting system $Oxyz$ and moves translationally together with the center of mass.

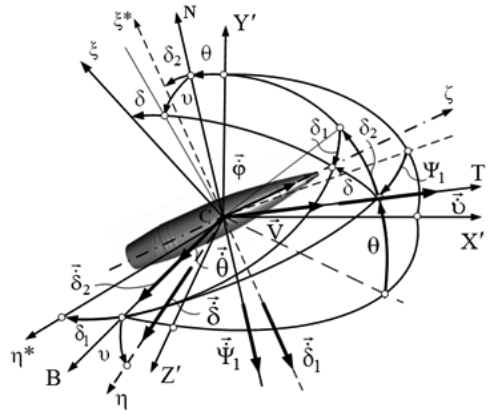


(a)

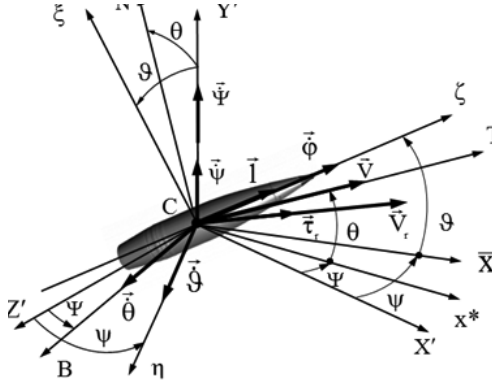


(b)

**Figure 1. Schemes of coordinate axes and angles.**

The position of the velocity vector of the center of mass of the projectile $\vec{V}$ in the starting coordinate system is found using the angle $\theta$ of inclination of the velocity vector to the horizon and the turning angle $\Psi_1$ of the velocity vector in the inclined plane, the positive direction of which is shown in Fig. 1. The position of the longitudinal axis of the projectile $\zeta$ relative to the velocity vector $\vec{V}$ of the center of mass is set in two ways. Using the Euler angles - the angles of precession $\nu$ and nutation $\delta$, using the Krylov angles $\delta_1$ and $\delta_2$[4,9]. The equations of motion of the center of mass and the equations of rotational motion relative to the center of mass are written in the trajectory system of axes $CTNB$. In this case, the values of the vector of the overturning aerodynamic moment $\vec{M}_s$ and the vector of the equatorial damping moment $\vec{M}_d$ as components of the total aerodynamic moment $\vec{M} = \vec{M}_s + \vec{M}_d$ are[4]:

$$M_s = q \cdot S \cdot L \cdot m_S(M_\infty, \delta);$$
$$M_{\vec{u}} = q \cdot S \cdot L \cdot m^{\bar{\omega}}(M_\infty, \delta) \cdot \bar{\omega}, \qquad (1)$$

where, q – velocity head of the oncoming air flow; S– projectile midship area; d –diameter of the projectile midship; L – length of the projectile; $\delta$ – nutation angle; $m_S(M_\infty, \delta)$ – dimensionless coefficient of the overturning aerodynamic moment, the values of which are determined depending on the angle of attack $\delta$ and the Mach number of the oncoming flow $M_\infty = V/a_\infty$; $a_\infty$ – is the sound velocity in the oncoming air flow; $m_i^{\bar{\omega}}$ – derivative of the coefficient of aerodynamic moment to the relative dimensionless angular velocity; $\bar{\omega} = \omega \cdot L / V$ – relative dimensionless angular velocity; $\omega$ – equatorial component of the angular velocity of the projectile; $V$ – the velocity of the center of the mass of the projectile.

At small angles $\delta_1$ and $\delta_2$, the system of linearized differential equations of the rotational motion of the projectile with respect to its center of mass in projections on the N and B axes of the trajectory system can be written in the form[4]:

$$\begin{aligned} \ddot{\delta}_1 + b \cdot \dot{\delta}_1 - g \cdot \dot{\delta}_2 + c \cdot \delta_1 + p \cdot \delta_2 &= \Delta_1 \\ \ddot{\delta}_2 + b \cdot \dot{\delta}_2 + g \cdot \dot{\delta}_1 + c \cdot \delta_2 - p \cdot \delta_1 &= \Delta_2 \end{aligned}, \qquad (2)$$

where,

$$b = f_2 + f_7;\ \ g = 2a;\ c = -f_4;\ a = (C/2A) \cdot r;$$
$$p = -2af_2;$$
$$\Delta_1 = -2a \cdot g \cdot V^{-1} \cdot \cos\theta;$$
$$\Delta_2 = -f_7 \cdot \dot{\theta} + g/V^2 \cdot \left[g \cdot \sin(2\theta) + f_1 \cdot \cos\theta\right];$$

r – angular velocity of rotation of the projectile relative to the longitudinal axis;
C– axial moment of inertia of the projectile;
A – equatorial moment of inertia of the projectile.

The relative values $f_1, f_2, f_4, f_7$ of the components of aerodynamic forces and moments ($f_1$ – longitudinal aerodynamic force; $f_2$ – transverse aerodynamic force; $f_4$ – overturning aerodynamic moment; $f_7$ – equatorial damping moment) are determined by the dependences:

$$f_1 = R_\zeta / m = q \cdot S \cdot C_\zeta / m = \frac{\pi \cdot \rho_{0N}}{8} \cdot \frac{d^2}{m} \cdot H(y) \cdot V_r^2 \cdot C_\zeta \left( \frac{V_r}{a_\infty}, \delta \right);$$

$$f_2 = R_{n\zeta} / (\delta \cdot m \cdot V_r) = q \cdot S \cdot C_{n\zeta} / (\delta \cdot m \cdot V_r) = \frac{\pi \cdot \rho_{0N}}{8} \cdot \frac{d^2}{\delta \cdot m} \cdot H(y) \cdot V_r \cdot C_{n\zeta} \left( \frac{V_r}{a_\infty}, \delta \right);$$

$$f_4 = M_s / (\delta \cdot A) = q \cdot S \cdot L \cdot m_S / (\delta \cdot A) = \frac{\pi \cdot \rho_{0N}}{8} \cdot \frac{d^2 \cdot L}{\delta \cdot A} \cdot H(y) \cdot V_r^2 \cdot m_s \left( \frac{V_r}{a_\infty}, \delta \right);$$

$$f_7 = M_{il} / (\omega \cdot A) = q \cdot S \cdot L \cdot m_M^{\bar{\omega}} \cdot \frac{L}{V} / A = \frac{\pi \cdot \rho_{0N}}{8} \cdot \frac{d^2 \cdot L^2}{A} \cdot H(y) \cdot V_r \cdot m^{\bar{\omega}} \left( \frac{V_r}{a_\infty}, \delta \right); \quad (3)$$

The quantities included in expression (3): $R_\zeta$ – longitudinal aerodynamic force; $R_{n\zeta}$ – transverse aerodynamic force; $V_r$ – velocity of the center of the mass of the projectile relative to the atmosphere, which is equal to the velocity of the oncoming flow; $C_\zeta, C_{n\zeta}$ – coefficients of longitudinal aerodynamic force and transverse aerodynamic force; $H(y)$ – function of atmospheric air density from altitude; m – mass of the projectile; $H(y) = \pi(y) \cdot \tau_{0N} / \tau$, where $\pi(y)$ – pressure function, $\tau_{0N}$ – temperature of the atmospheric air under normal terrestrial conditions; $\tau$ – temperature at the calculated point of the trajectory. The notations adopted in[4] is retained.

Expression (1) for the equatorial aerodynamic damping moment $M_d$ contains the derivative of the aerodynamic moment coefficient to the relative dimensionless angular velocity $\bar{\omega}$. Let us consider possibility of quantitatively estimating the value of the equatorial damping moment for an axisymmetric rotation body, using the results of numerical calculations of the overturning aerodynamic moment coefficient $m_s(M_\infty, \delta)$, the values of which are determined depending on the angle of attack $\delta$ and the Mach number of the oncoming air flow $M_\infty = V / a_\infty$. The presence of the equatorial angular velocity of the rotation body leads to a change in the local angles of attack and normal forces on its surfaces (Fig. 2).

The appearance of additional local angles of attack leads to the appearance of additional elementary normal aerodynamic forces and moments, which are a consequence of the presence of the angular velocity of rotation. An additional value of the aerodynamic moment, depending on the angular velocity of rotation of the body, is the damping moment:

$$M_d = \left( \frac{dM_S}{d\delta} \right)_0 \cdot d\delta_\omega + \left( \frac{dM_S}{d(M_\infty)} \right)_0 \cdot d(M_\infty)_\omega \quad (4)$$

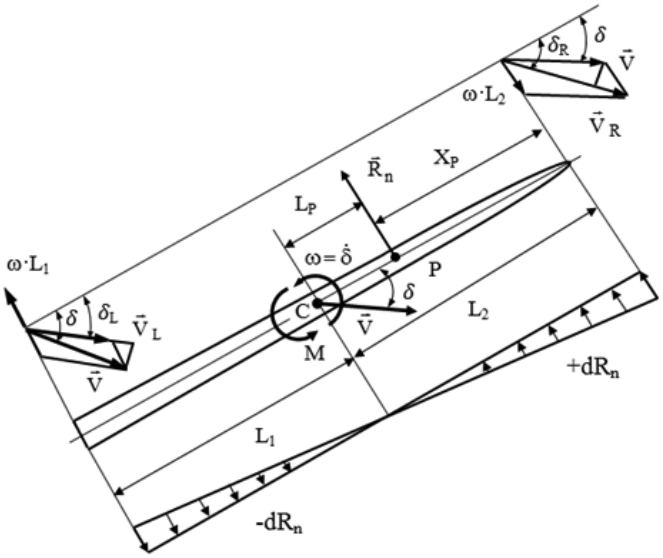


**Figure 2. Elementary local angles of attack δR,δL and normal forces ±dRn during rotation of the body in the oncoming flow with the angle of attack δ.**

We assume that the equivalent elementary increment in the angle of attack $d\delta_\omega$ of all points of the surface of the rotation body, averaged over the body length, is equal to the average value of the range of variation in the angle of attack due to the presence of the rotational velocity of points on the surface of the rotation body:

$d\delta_\omega = 0.5 \cdot d\delta_\Sigma = 0.5 \cdot (d\delta_L + d\delta_R)$; $d\delta_L = \delta - \delta_L$;
$d\delta_R = \delta_R - \delta$ (Fig. 2). In this case:

$$d\delta_L = \frac{\dot{\delta} \cdot L_1 \cdot \cos\delta}{V}; \; d\delta_R = \frac{\dot{\delta} \cdot L_2 \cdot \cos\delta}{V}; \; d\delta_\omega = 0.5 \cdot \frac{\dot{\delta} \cdot L}{V} \cdot \cos\delta \quad (5)$$

Similarly, we find the elementary increment in the Mach number in the oncoming air flow $d(M_\infty)_\omega$, averaged over the body length, due to the presence of the rotational velocity of points on the body surface:

$$d(M_\infty)_\omega = \frac{0.5 \cdot \omega}{a_\infty} \cdot L \cdot \sin\delta = \frac{0.5 \cdot L}{a_\infty} \cdot \sin\delta \cdot \dot{\delta} \quad (6)$$

Determining the necessary derivatives and substituting them together with (5) and (6) in (4), we will have the following expression for the damping moment $M_d$ and the damping moment coefficient $f_7 = M_d / (\dot{\delta} \cdot A)$ in Eqns. (2) ($\sin\delta \approx \delta$, $\cos\delta \approx 1$, $\omega_i = \dot{\delta}$):

$$M_d = 0.25 \rho S L^2 \left\{ V \left( \frac{dm_s}{d\delta} \right)_0 + a\delta \left[ \left( \frac{dm_S}{d(M_\infty)} \right)_0 \cdot M_\infty^2 + 2M_\infty \cdot m_S \right] \right\} \dot{\delta}$$

$$f_7 = \frac{0.25\rho S L^2}{A}\left\{V\left(\frac{dm_s}{d\delta}\right)_0 + a\delta\left[\left(\frac{dm_S}{d\left(M_\infty\right)}\right)_0 \cdot M_\infty^2 + 2M_\infty \cdot m_S\right]\right\} \tag{7}$$

The decrease in the angular velocity $r$ of rotation of the projectile relative to its longitudinal axis as a result of the action of the moment of surface friction was determined by the theoretical Slezkine's formula[4]:

$$r = r_0 \cdot e^{-0.598 \cdot \frac{d \cdot t^{4/5}}{2q} \cdot \int V^{4/5} \cdot dt},$$

where $r_0$ – initial angular velocity; $d$ – the diameter of the projectile amidships; q – weight of the projectile; V – flight velocity; t – flight time

If we consider as the unperturbed rotational motion of the artillery projectile, the rotational motion, in which $\delta_1 = 0;$ $\delta_2 = 0;\ \dot{\delta}_1 = 0;\ \dot{\delta}_2 = 0$, then the system of equations of the perturbed rotational motion of the first approximation is obtained from the system of linearized Eqns. (2) by zeroing the right-hand sides and reducing the resulting system of homogeneous differential equations to the canonical form:

$$\begin{aligned} &\dot{\delta}_1 = \varepsilon_1; \quad \dot{\varepsilon}_1 = -b \cdot \dot{\delta}_1 + g \cdot \dot{\delta}_2 - c \cdot \delta_1 - p \cdot \delta_2; \\ &\dot{\delta}_2 = \varepsilon_2; \quad \dot{\varepsilon}_2 = -b \cdot \dot{\delta}_2 - g \cdot \dot{\delta}_1 - c \cdot \delta_2 + p \cdot \delta_1. \end{aligned} \tag{8}$$

The characteristic equation of the system of differential equations of the first approximation takes the form:

$$\begin{aligned} &D(\lambda) = \lambda^4 + 2b_\tau\lambda^3 + (g_\tau^2 + b_\tau^2 + 2c_\tau)\cdot\lambda^2 + (c_\tau b_\tau - g_\tau p_\tau)\cdot 2\lambda + c_\tau^2 + p_\tau^2 = 0 \\ &b_\tau = b/\nu; \qquad g_\tau = g/\nu; \qquad c_\tau = c/\nu^2; \qquad p_\tau = p/\nu^2 \end{aligned} \tag{9}$$

We introduced a dimensionless time $\tau = \nu \cdot t$, where $\nu$ is the parameter with the dimension of frequency (1/s). In this case, the system of differential Eqns. (2) will contain derivatives by the dimensionless time. Substituting the imaginary number $\lambda = j\omega$ in (9), we obtain the complex frequency function ( $\omega$ – frequency parameter):

$$D(j\omega) = X(\omega) + j \cdot Y(\omega), \tag{10}$$

where,

$$\begin{aligned} &X(\omega) = \omega^4 - (g_\tau^2 + b_\tau^2 + 2c_\tau)\cdot\omega^2 + (c_\tau^2 + p_\tau^2); \\ &Y(\omega) = -2\cdot[b_\tau \cdot \omega^3 + \omega\cdot(g_\tau \cdot p_\tau - c_\tau \cdot b_\tau)] \end{aligned}$$

The computational model[4], adopted for writing Eqns. (2) of the perturbed rotational motion of the projectile relative to its center of mass, does not provide for the presence of wind. At the same time, it is known that the wind has a significant effect on the flight of the projectile both in the longitudinal and lateral directions. Let us consider an alternative system of equations for the perturbed rotational motion of the projectile and write the right-hand sides of the equations of the system in a form that allows us to apply them in the presence of wind disturbances. The equations of the perturbed rotational motion of the projectile relative to its center of mass in projections on the axes of a semi-connected system of axes $C\zeta\xi\eta$, obtained on the basis of the dynamic equations of Euler's rotational motion, can be written in the form[4]:

$$\begin{aligned} &A\cdot\left(\ddot{\psi}\cdot\cos\vartheta - 2\cdot\dot{\psi}\cdot\dot{\vartheta}\cdot\sin\vartheta\right) + C\cdot\dot{\vartheta}\cdot(\dot{\phi} + \dot{\psi}\cdot\sin\vartheta) = \sum_n^{i=1} M_{\xi i}; \\ &A\cdot\left(\ddot{\vartheta} + \dot{\psi}^2\cdot\cos\vartheta\cdot\sin\vartheta\right) - C\cdot\dot{\psi}\cdot(\dot{\phi} + \dot{\psi}\cdot\sin\vartheta)\cdot\cos\vartheta = \sum_n^{i=1} M_{\eta i} \end{aligned} \tag{11}$$

where $\psi$ – the yaw angle of the projectile axis in the starting coordinate system; $\vartheta$ – the pitch angle of the projectile axis in the starting coordinate system; $\phi$ – the angle of rotation of the projectile around the longitudinal axis (Fig. 1(b)).

The right-hand sides of Eqns. (11) contain the moments of the forces acting on the projectile relative to the axes $\xi$ and $\eta$. The moments of the gravity $m\vec{g}$ and of the longitudinal aerodynamic force $\vec{R}_\zeta$, provided that there are no corresponding eccentricities, are equal to zero. Consider the action of the aerodynamic overturning moment $\vec{M}_s$. In the presence of wind, the vector of the velocity of the center of mass relative to the atmosphere $\vec{V}_r = \vec{V} - \vec{W}$, where $\vec{V}$ – the vector of the absolute velocity of the center of mass of the projectile, $\vec{W}$ – the vector of the wind velocity. The line of direction of the velocity vector $\vec{V}_r$ and the axis of the projectile $\zeta$ form a plane, which is commonly called the resistance plane (Fig. 3(a)). In this plane, the main components of aerodynamic forces and moments operate. The transverse aerodynamic force $\vec{R}_{n\zeta}$ acts in the plane of resistance of the projectile at point D (Fig. 3(a)), which is commonly called the center of pressure, and creates the overturning aerodynamic moment. We write the vector of this moment $\vec{M}_s$ using the unit vector $\vec{l}$ of the projectile axis and the unit vector $\vec{\tau}_r$ in the direction of the relative airspeed $\vec{V}_r$ of the projectile center of mass (Fig.3(a)):

$$\begin{aligned} &\vec{M}_s = M_s / \bar{m}\cdot\left(\vec{\tau}_r \times \vec{l}\right), \\ &M_s = m_s\left(\delta, M_\infty\right)\cdot q\cdot S\cdot L \end{aligned} \tag{12}$$

where $m_s\left(\delta, M_\infty\right)$ – dimensionless coefficient of the aerodynamic overturning moment, determined from the results of aerodynamic calculations or tests, depending on the angle of attack $\delta$ and the Mach number $M_\infty$ of the incoming flow; $q = \rho V_r^2/2$ – velocity head of the oncoming air flow; S – the projectile midsection area; L – the length of the projectile, $= \left|\mathrm{mod}\left(\vec{\tau}_r \times \vec{l}\right)\right| = \left|\sin\delta\right.$ – module of the vector multiplication of vectors $\vec{\tau}_r$ and $\vec{l}$ ;

To find the projections of the aerodynamic overturning moment vector $\vec{M}_s$ on the axes of the semi-connected system $C\zeta\xi\eta$, we write the product of vectors $(\vec{l}\times\vec{\tau}_r)$ in the semi-connected system of axes using a well-known determinant.

Expanding the determinant, we have the following values of the projections of the aerodynamic overturning moment on the axes of the semi-connected system:

$$M_\zeta = M_s / \bar{m}\left(l_\eta \tau_{r\xi} - l_\xi \tau_{r\eta}\right); M_\xi = M_s / \bar{m}\left(l_\zeta \tau_{r\eta} - l_\eta \tau_{r\zeta}\right)$$
$$M_\eta = M_s / \bar{m}\left(l_\xi \tau_{r\zeta} - l_\zeta \tau_{r\xi}\right) \quad (13)$$

Since the projections of the unit vector $\vec{l}$ onto the semi-connected axes $C\zeta\xi\eta$ have obvious values $l_\zeta = 1$, $l_\xi = 0$, $l_\eta = 0$, then expressions (13) for the moments are simplified:

$$M_\zeta = 0; \quad M_\xi = M_s / \bar{m} \cdot \tau_{r\eta}; \quad M_\eta = -M_s / \bar{m} \cdot \tau_{r\xi} \quad (14)$$

We find the projections $\tau_{r\eta}$ and $\tau_{r\xi}$ of the unit vector $\vec{\tau}_r$ on the axes of the semi-connected system $C\zeta\xi\eta$. For this, we project the vector equality $\vec{V}_r = \vec{V} - \vec{W}$ on the x,y,z axes of the starting system. As a result, we get the projections of the vector $\vec{\tau}_r$ onto these axes in the presence of wind: $\tau_{rx} = (\dot{x}_c - W_x)/V_r$; $\tau_{ry} = (\dot{y}_c - W_y)/V_r$; $\tau_{rz} = (\dot{z}_c - W_z)/V_r$, where: $x_c, y_c, z_c$ – coordinates of the center of mass of the projectile in the starting coordinate system; $V_r = \sqrt{(\dot{x}_c - W_x)^2 + (\dot{y}_c - W_y)^2 + (\dot{z}_c - W_z)^2}$, $W_x, W_y, W_z$ – wind components in the direction of the x, y, z coordinate axes of the starting system.

Using the known coordinate transformation, we find the projections $\tau_{r\xi}$ and $\tau_{r\eta}$:

$$\tau_{r\xi} = -\tau_{rx} \cdot \sin\vartheta \cdot \cos\psi + \tau_{ry} \cdot \cos\vartheta + \tau_{rz} \cdot \sin\vartheta \cdot \sin\psi$$
$$\tau_{r\eta} = \tau_{rx} \cdot \sin\psi + \tau_{rz} \cdot \cos\psi \quad (15)$$

To analyze the precessional rotational motion of the projectile axis, one can use the projections of the unit vector $\vec{l}$ on the axes of the CTNB trajectory system (Fig. 1(b)). At small angles of nutation, we can assume that $l_B = \delta_1$ and $l_N = \delta_2$. Taking into account that the projections of the unit vector $\vec{l}$ on the axes of the semi-connected system of axes $C\zeta\xi\eta$ have obvious values $l_\zeta = 1$, $l_\xi = 0$, $l_\eta = 0$, and making the transition to the starting coordinate system, we obtain the values of the projections of the unit vector $\vec{l}$ on the axes of the starting coordinate system in the form: $l_x = \cos\vartheta \cdot \cos\psi$; $l_y = \sin\vartheta$; $l_z = -\cos\vartheta \cdot \sin\psi$.

Now we find the projections of the unit vector $\vec{l}$ on the axes of the trajectory coordinate system, using the well-known transition formulas:

$$l_T = l_x \cdot \cos\theta \cdot \cos\Psi + l_y \cdot \sin\theta - l_z \cdot \cos\theta \cdot \sin\Psi;$$
$$l_N = -l_x \cdot \sin\theta \cdot \cos\Psi + l_y \cdot \cos\theta + l_z \cdot \sin\theta \cdot \sin\Psi;$$
$$l_B = l_x \cdot \sin\Psi + l_z \cdot \cos\Psi \quad (16)$$

The obtained values of the projections $l_B = \delta_1$ and $l_N = \delta_2$ can be used for numerical and visual graphical analysis of the precessional rotational motion of the projectile axis in an undisturbed atmosphere and in the presence of wind.

The system of Eqns. (2), (11) of the rotational motion of the projectile relative to the center of mass is supplemented by the well-known equations of motion[1,2,4] of the center of mass. In particular, the kinematic equations of motion of the center of mass in projections on the axes of the starting coordinate system and the dynamic equations of motion of the center of mass in projections on the axes of the trajectory coordinate system have the form[4]:

$$1)\ \dot{y}_c = V \cdot \sin\theta;\ 2)\ \dot{x}_c = V \cdot \cos\theta \cdot \cos\Psi;\ 3)\ \dot{z}_c = -V \cdot \cos\theta \cdot \sin\Psi;$$
$$4)\ \dot{V} = \Sigma F_T / m;\ 5)\ \dot{\theta} = \Sigma F_N / (m \cdot V);\ 6)\ \dot{\Psi} = -\Sigma F_B / (m \cdot V \cdot \cos\theta), \quad (17)$$

where $x_c, y_c, z_c$ – coordinates of the center of mass of the rotation body in the starting coordinate system; $\theta$ and $\Psi$ are the velocity angles of pitch and yaw, which determine the direction of the velocity vector $\vec{V}$ of the center of mass of the projectile in the starting coordinate system; m is the mass of the projectile; $\Sigma F_T, \Sigma F_N, \Sigma F_B$ are the sums of the projections of forces on the axes of the CTNB trajectory system. When finding the projections of the longitudinal aerodynamic force $\vec{R}_\zeta$ and transverse aerodynamic force $\vec{R}_{n\zeta}$, it is convenient to use the vector expressions: $\vec{R}_\zeta = -R_\zeta \cdot \vec{l}$; $\vec{R}_{n\zeta} = R_{n\zeta} / \bar{m} \cdot [\vec{l} \times (\vec{l} \times \vec{\tau}_r)]$.

Ballistic calculations were preceded by aerodynamic calculations of the flow around an axisymmetric rotation body of the 155-mm caliber artillery projectile type with a «cone-cone-ogive» head part in the interval of sub-, trans-, and supersonic flow velocities in the presence of angles of attack according to the drawing of its external contours. The approximate dimensions of the outer contours of the artillery shell were taken from the study.[7] According to these approximate dimensions, the sketch of the external contours of the projectile was developed, which was used for calculations.

As a result of the calculations, the values of the aerodynamic longitudinal force $R_\zeta$, the aerodynamic transverse force $R_{n\zeta}$, the coordinates of the center of pressure and the values of the overturning aerodynamic moment $M_s$ relative to the center of mass (Fig. 3(a)) were obtained with the subsequent calculation of the coefficients of the aerodynamic forces and the moment in accordance with dependencies (1) and (3) at the number of values of the angle of attack within the limits $0 \le \delta \le 6^0$ and Mach numbers of the oncoming flow $0.1 \le M_\infty \le 3.0$. Calculations of aerodynamic forces, overturning moment and their coefficients were performed by numerically solving of the Reynolds-averaged Navier-Stokes equations using the ANSYS CFX software package. Aerodynamic coefficients were calculated as functions of the Mach number $M_\infty$ and the angle of attack

$\delta$. In Fig. 3(b) shows the dependence of the coefficient $m_s$ of the aerodynamic overturning moment for the angle of attack $\delta = 2.0^0$ on the freestream Mach number $M_\infty$.

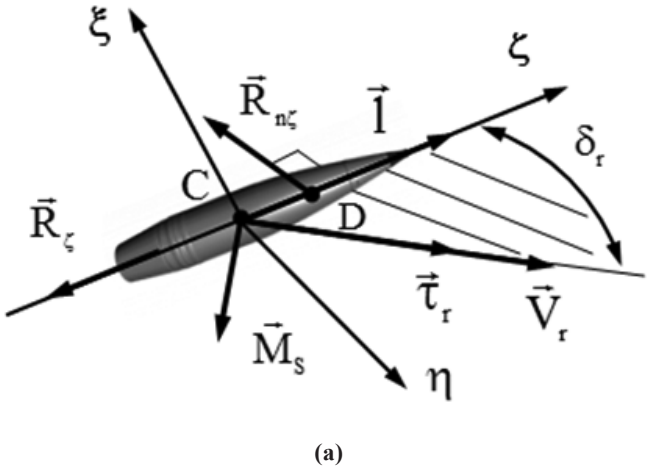


**(a)**

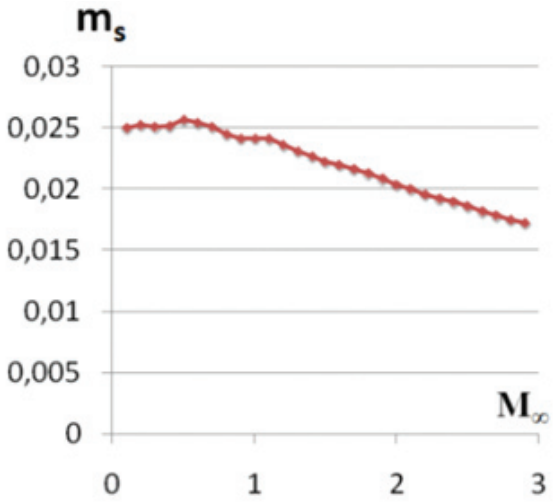


**(b)**

**Figure 3. (a) Resulting aerodynamic forces and overturning moment in the drag plane, (b) Calculated dimensionless coefficient $m_S$ for overturning moment $M_S$.**

## 3. RESULTS AND DISCUSSION

### 3.1 Analysis of Stability of Rotational Motion of Projectile Based on Mikhailov's Frequency Criterion[10]

The parameters of the flight trajectory and angular displacements of the projectile along the trajectory were calculated by numerical integration of the system of differential Eqns. (2), (11) and (17). The calculation of the parameters of the Mikhailov curve was carried out according to dependence (10) for the complex frequency function. Ballistic calculations were performed with the projectile mass m = 42.0 kg, the equatorial moment of inertia $A = 1.95\ kg \cdot m^2$, the axial moment of inertia $C = 0.35\ kg \cdot m^2$, the initial projectile velocity $V_0$ = 900 m/s and the elevation angle of the gun $\theta_0 = 35^0$. The system of differential equations was solved numerically by the Runge-Kutta method of the 4th order under initial conditions $\delta_{10} \neq 0$; $\delta_{20} \neq 0$; $\dot{\delta}_{10} = 0$; $\dot{\delta}_{20} = 0$. The frequency parameters were as follows: $\nu = 10\ s^{-1}$, $\omega = 0 \div 200$. In Fig. 4(a) shows the results of calculations of the Mikhailov curve at the end of the first two seconds of flight.

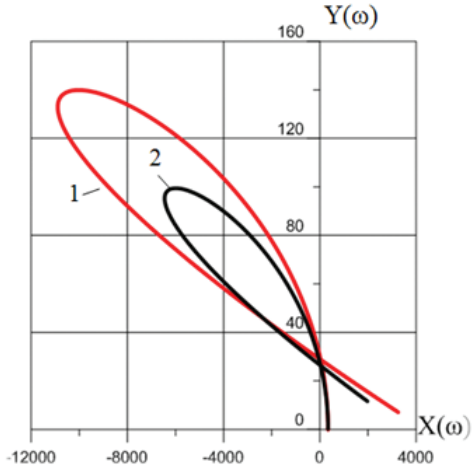


**(a)**

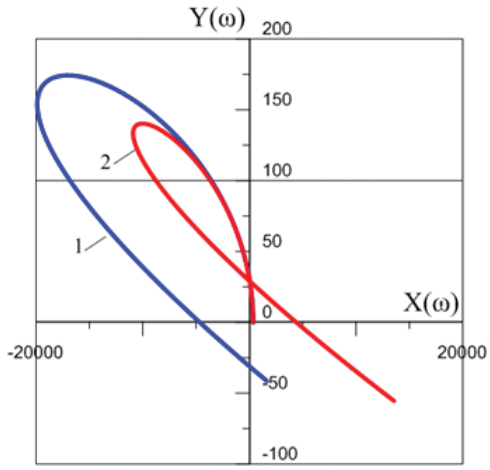


**(b)**

**Figure 4. Mikhailov curves for the projectile: (a) at overturning aerodynamic moment (1 – $r_0$ = 1800 rad/s; 2 – $r_0$ =1440 rad/s); (b) 1 – at restoring aerodynamic moment; 2 – at overturning aerodynamic moment ($r_0$ = 1800 rad/s)**

Curve 1 corresponds to the initial angular velocity of rotation of the projectile around the longitudinal axis $r_0$ = 1800 rad/s, curve 2 – reduced by 20 % angular velocity $r_0$ (1440 rad/s). It can be seen that curves 1 and 2, starting their motion on the real positive semiaxis and rotating only counterclockwise, pass sequentially only two quadrants of the coordinate plane at the fourth degree of the characteristic equation. According to Mikhailov's criterion, this indicates the asymptotic instability of the rotational motion of the projectile on the flight trajectory.

To verify the correctness of using the Mikhailov criterion for assessing the stability of the rotational motion of the projectile, a comparative analysis of the results of calculating the Mikhailov curve for overturning and stabilizing moments was carried out by changing the sign of the aerodynamic moment coefficient $f_4$. In Fig. 4(b) shows Mikhailov curves for these two cases at

$r_0$ = 1800 rad/s. Curve 1 corresponds to an aerodynamically stabilized projectile. Curve 2 repeats curve 1 in Fig. 4(a) for an aerodynamically unstabilized projectile. It can be seen that in the case of an aerodynamically stabilized projectile, the Mikhailov curve (Fig. 4(b), curve 1), starting its motion on the real positive semiaxis and rotating only counterclockwise, successively passes through four quadrants of the coordinate plane at the fourth degree of the characteristic equation, which, according to the Mikhailov criterion, indicates asymptotic stability of the rotational motion of the projectile on the flight trajectory.

### 3.2 Comparative Analysis of Characteristics of Perturbed Rotational Movement of Projectile on Flight Trajectory

In accordance with the purpose of this work, a computational study of the characteristics of the disturbed rotational motion of a gyroscopically stabilized and dynamically balanced artillery projectile was carried out in individual sections of the flight trajectory in the presence of the following disturbances: the initial deviation of the projectile axis from the direction of motion, changes in the initial rotation velocity projectile, changes in the elevation angle of the gun barrel, the presence of wind. The values of the angles and components of the equatorial angular velocities of the rotational motion of the projectile when exiting the gun barrel, used in the calculations, were taken on the basis of the experimental data given in[11,12].

Part of the performed calculations was devoted to studying the influence of the conditions of projectile departure from the gun barrel on its perturbed precessional motion. The main characteristics of the perturbed rotational motion are the angles $\delta_1$ and $\delta_1$.

Below are some calculated graphical dependences for the angles $\delta_1$, $\delta_2$, obtained on the calculated flight trajectory. The two dependences $\delta_2 = f(\delta_1)$ shown in Fig. 5(a) were obtained for total flight time at $V_0 = 930$ m/s, $r_0$=1860 rad/s, $\theta_0 = 45^0$, $\delta_{10} = \delta_{20} = 0.1$ deg., $\dot{\delta}_{10} = \dot{\delta}_{20} = 0.15\ rad/s$. Dependence 1 (black color) was obtained without taking into account, dependence 2 (red color) – taking into account the equatorial damping moment. The two dependences $\delta_2 = f(\delta_1)$ shown in Fig. 5(b) were obtained for total flight time at $\theta_0 = 45^0$, $V_0 = 325$ m/s, $r_0$=650 rad/s, $\delta_{10} = \delta_{20} = 0.15$ deg., $\dot{\delta}_{10} = \dot{\delta}_{20} = 0.35\ rad/s$. It can be seen that a decrease in the departure velocity $V_0$ and the initial angular velocity of the projectile $r_0$ led to a noticeable increase in the periodic components of the angles $\delta_1$ and $\delta_2$ with a significant decrease in their non-periodic components (components of the dynamic equilibrium angle). As in the previous figures, dependence 1 (black color) was obtained without taking into account, dependence 2 (red color) – taking into account the equatorial damping moment. The two dependences $\delta_2 = f(\delta_1)$ shown in Fig. 5(c) were obtained in the time interval 3÷10 seconds of flight at $\theta_0 = 35^0, V_0 = 930$ m/s, $r_0$=1860 rad/s, $\delta_{10} = \delta_{20} = 0.1$ deg., $\dot{\delta}_{10} = \dot{\delta}_{20} = 0.15\ rad/s$. As in the previous figures, one can see a decrease in the periodic components of the angles $\delta_1$ and $\delta_2$ when calculated taking into account the equatorial damping moment. In Fig. 5(d) shows the calculated dependences $\delta_2 = f(\delta_1)$ along the trajectory without taking into account and taking into account the equatorial damping moment at $\theta_0 = 35^0$, $V_0 = 930$ m/s, $r_0$=1860 rad/s, $\delta_{10} = \delta_{20} = 0.15$ deg., $\dot{\delta}_{10} = \dot{\delta}_{20} = 0.35\ rad/s$. In Fig. 5(e) shows the calculated dependences of the angle $\delta_1$ on the time T for this case. It can be seen that an increase in the initial values of the angles $\delta_{10}$, $\delta_{20}$ and the initial components $\dot{\delta}_{10}$, $\dot{\delta}_{10}$ of the equatorial angular velocity of the projectile led to a noticeable increase in the influence of the equatorial damping moment on the periodic component of the angle $\delta_1$, especially on the descending part of the trajectory**.** At the same time, there was a decrease in the non-periodic component of the angle $\delta_1$ compared to the result in Fig. 5(a), which can be explained by the decrease in the elevation angle from $\theta_0 = 45^0$ to $\theta_0 = 35^0$. For clarity, in Fig. 5(e) shows the calculated dependences of the angle $\delta_1$ on time T for a short time interval at the end of the descending section of the trajectory.

### 3.3 Loss of Stability at Changes in the Initial Rotation Velocity Projectile

As known, a decrease in the initial velocity of rotation of the projectile can lead to a loss of stability of its rotational motion along the flight trajectory. In this work, the calculated loss of stability occurred taking into account the action of the equatorial damping moment at the initial section of the trajectory with a decrease in the initial rotation velocity from $r_0$ = 1860 rad/s (Fig. 5(a)) to $r_0$ = 1130 rad/s while maintaining the exit velocity from the gun barrel $V_0$ = 930 m/s , initial values $\delta_{10} = \delta_{20} = 0.1$ deg., $\dot{\delta}_{10} = \dot{\delta}_{20} = 0.15\ rad/s$ and the elevation angle of the gun barrel $\theta_0 = 45^0$. In Fig. 6 the results of calculations of the spatial nutation angle components are presented in the form of the dependence $\delta_2 = f(\delta_1)$ (Fig. 6(a), Fig. 6(b), Fig. 6(c)) and dependence of the gyroscopic stability coefficient $\sigma = 1 - f_4/a^2$ on the flight time T (Fig. 6(d)), where $a = (C \cdot r)/(2A)^4$, obtained along the trajectory at different initial angular velocities of the projectile. This criterion is effective in the initial section of the trajectory.[4]

It can be seen that as the initial rotation velocity decreases, the non-periodic components of the nutation angle decreased and its periodic components increased. In this case, the criterion of gyroscopic stability $\sigma = 1 - f_4/a^2$ at the initial part of the trajectory gradually approached the condition $\sigma < 0$.

Figure 6(c) shows the calculated dependence $\delta_2 = f(\delta_1)$ obtained at the initial angular velocity of the projectile $r_0$ = 1130 rad/s in the calculated time interval of 0.5 second from the moment of departure. A sharp increase in the nutation angle can be seen, leading to the breakdown of the precessional motion of the projectile axis at the time T=0.49 seconds from the moment of departure. Fig. 6(d) shows the calculated time T dependence of the gyroscopic stability criterion $\sigma$ for this case. The given dependence shows that the condition of gyroscopic stability of a rotating projectile $\sigma = 1 - f_4/a^2 > 0$ is not satisfied,

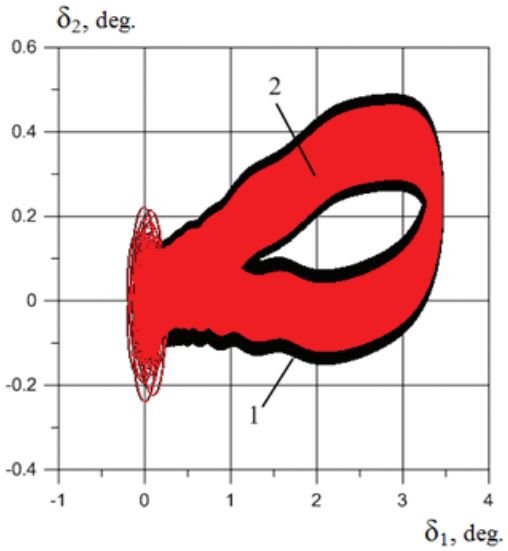


(a) $\Theta_0=45^0$; $V_0=930$ m/s; $r_0=1860$ c$^{-1}$; $\delta_0=0.1$; $\dot{\delta}_0 = 0.15$ c$^{-1}$.

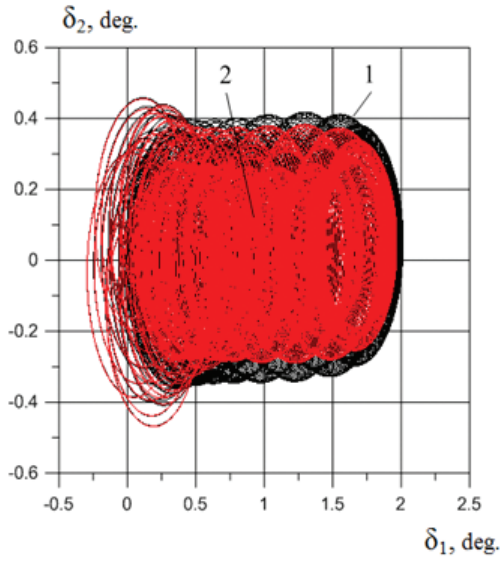


(b) $\Theta_0=45^0$; $V_0=325$ m/s; $r_0=650$ c$^{-1}$; $\delta_0=0.1$; $\dot{\delta}_0 = 0.35$ c$^{-1}$.

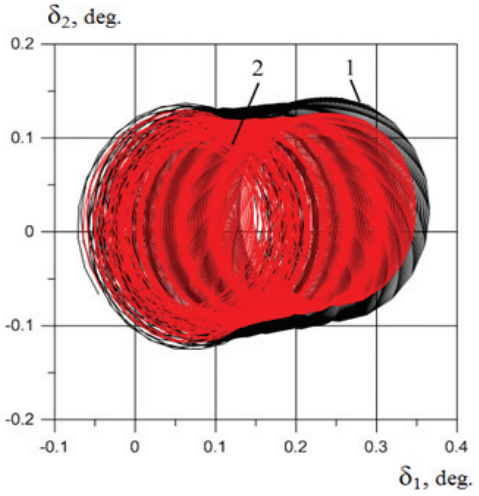


(c) $\Theta_0=35^0$; $V_0=930$ m/s; $r_0=1860$ c$^{-1}$; $\delta_0=0.1$; $\dot{\delta}_0 = 0.15$ c$^{-1}$.

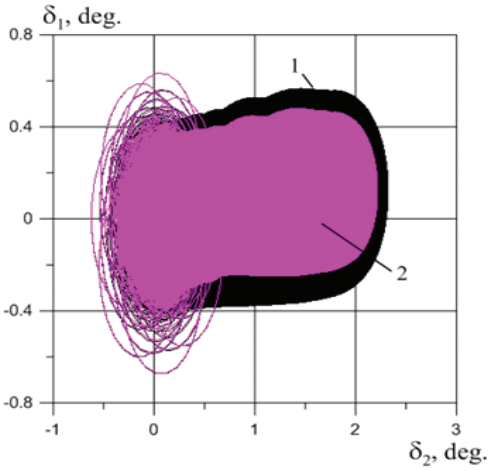


(d) $\Theta_0=35^0$; $V_0=930$ m/s; $r_0=1860$ c$^{-1}$; $\delta_0=0.15$; $\dot{\delta}_0 = 0.35$ c$^{-1}$.

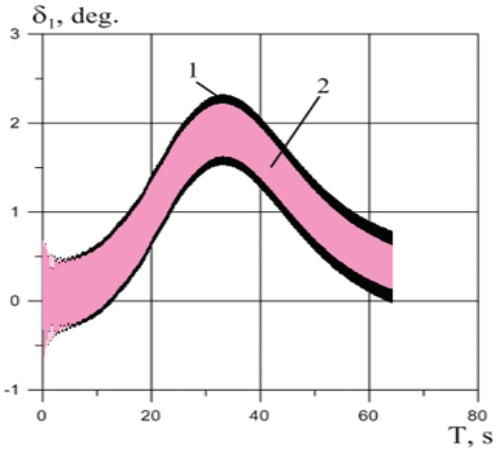


(e) $\Theta_0=35^0$; $V_0=930$ m/s; $r_0=1860$ c$^{-1}$ ; $\delta_0=0.15$; $\dot{\delta}_0 = 0.35$ c$^{-1}$.

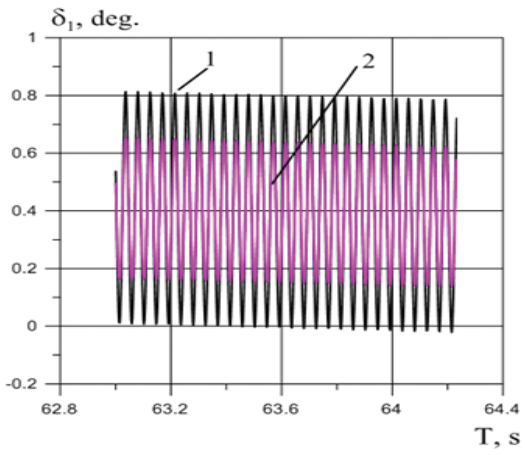


(f) $\Theta_0=35^0$; $V_0=930$ m/s; $r_0=1860$ c$^{-1}$;$\delta_0=0.15$; $\dot{\delta}_0 = 0.35$ c$^{-1}$.

**Figure. 5. Dependences for angles δ1 and δ2 on the flight trajectory: 1 – without equatorial damping moment; 2 – taking into account the equatorial damping moment.**

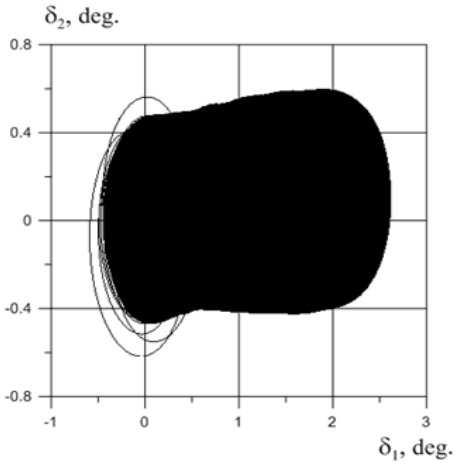


(a) Total flight time, $r_0$ = 1260 rad/s

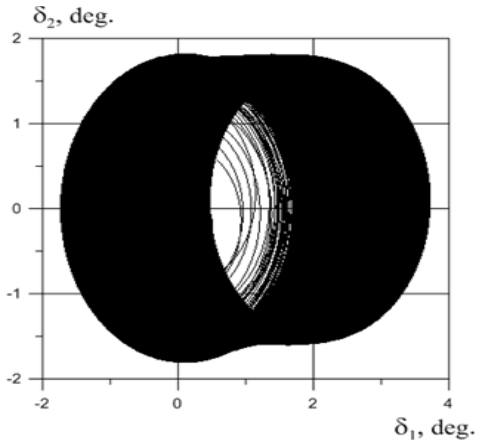


(b) Total flight time, $r_0$ = 1170 rad/s

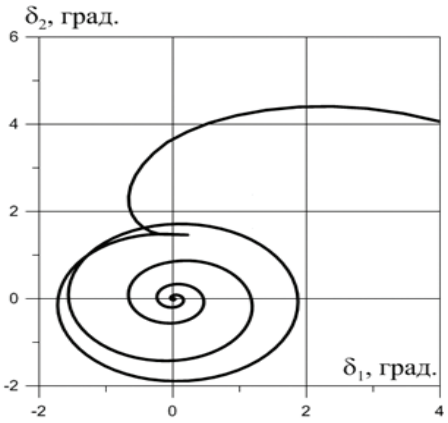


(c) 0.5 seconds of flight, $r_0$ = 1130 rad/s

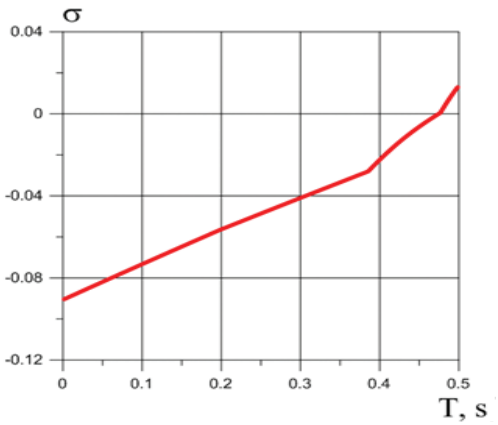


(d) 0.5 seconds of flight, $r_0$ = 1130 rad/s

**Figure 6. Dependences demonstrating the loss of stability of the rotational movement of the projectile with a decrease in the initial rotation velocity ($V_0$ = 930 m/s, $\Theta_0$=45⁰).**

starting from the moment of departure. The calculation results obtained above show that the condition of gyroscopic stability of a rotating projectile $\sigma = 1 - f_4/a^2 > 0$, obtained by N. V. Maievsky in the absence of trajectory curvature and given in[4], can be applied at the initial segment of trajectory.

### 3.4 Loss of Stability with Increasing Elevation Angle

In the case considered above, the loss of stability of the rotational movement of the projectile occurred immediately after the projectile exited the gun barrel at a constant elevation angle of the barrel, a constant departure velocity and a sequential decrease in the initial angular velocity of rotation. At the same time, it is known that as the curvature of the trajectory increases, the dynamic equilibrium axis of the rotating projectile deviates more and more from the velocity vector of its center of mass[1 - 4]. This leads to an increase in the spatial angle of attack of the oncoming flow and can cause loss of stability of the rotational motion of the projectile on steep trajectories (Fig. 7). In Fig. 7(a) shows the calculated dependence $\delta_2 = f(\delta_1)$ at an elevation angle of 45⁰, the exit velocity $V_0$ = 330 m/s and the initial angular velocity $r_0$ = 650 rad/s. In Fig. 7(b) for comparison shows similar calculated dependence at the same velocities and an elevation angle of $\theta_0 = 50^0$. One can see a significant increase in the angle $\delta_1$ in the upper part of the trajectory at angle of $\theta_0 = 50^0$. A further increase of the elevation angle while maintaining the initial velocity $V_0$=330 m/s and the initial angular rotation velocity $r_0$=650 rad/s led to the calculated loss of stability in the region of the upper point of the trajectory, starting from the elevation angle $\theta_0 = 60^0$. It should be noted that the stability condition of a rotating projectile $\sigma = 1 - f_4/a^2 > 0$ was obtained for movement on a straight section of the trajectory and should not be applied for the section of the trajectory in the region of the top. The independent calculated criterion evaluating the stability of rotating projectiles on a curved section of the trajectory can be the angle $\delta_1$[4]. Fig. 7(c) corresponds to the time interval from the moment of departure to the moment of loss of stability of the rotational motion in the region of the upper point of the trajectory on its descending branch at the moment of flight T ≈ 24.2 s. It can be seen that at the moment of loss of stability, the angle $\delta_1$ reaches the value $\approx 6.0^0$. With a further increase in the elevation angle of the gun barrel, the loss of stability occurs

earlier. Fig. 7(d) corresponds to the elevation angle $\theta_0 = 65^0$ and the time interval from the moment of departure to the moment of loss of stability of rotational motion when approaching the upper point of the trajectory along its ascending branch during the flight T = 21.9 s

Further calculation was performed at the angle $\theta_0 = 70^0$. In this case, the initial velocity and the initial angular velocity of rotation were respectively $V_0$=930 m/s and $r_0$=1860 rad/s. During the first calculation, the initial parameters of the rotational motion were: $\delta_{10} = \delta_{20} = 0.15$ deg., $\dot{\delta}_{10} = \dot{\delta}_{20} = 0.35\ rad/s$. The projectile lost stability of rotational motion on the ascending branch of the trajectory when approaching its upper point during the flight T=31.93 s. In Fig. 7(e) shows two dependences. As before, number 1 denotes the result of the calculation without the equatorial damping moment, number 2 – with the equatorial damping moment. In the second calculation, the initial parameters of the rotational motion were: $\delta_{10} = \delta_{20} = 0.15$ deg., $\dot{\delta}_{10} = \dot{\delta}_{20} = 1.5\ rad/s$. In Fig. 7(f) shows the results of this calculation. One can see an increase in the periodic components of the angular displacements of the projectile, caused by an increase in the components of the initial equatorial angular velocity, with a simultaneous noticeable increase in the influence of the damping moment on the amplitude of the angular oscillations of the projectile. At the same time, the non-periodic components of the angles $\delta_1$ and $\delta_2$, which determine the angle of dynamic equilibrium, did not change noticeably. A slight decrease in time until the moment of loss of stability from 31.93 seconds to 31.09 seconds was recorded.

### 3.5 Wind Influence

All previous calculations were consistent with a stationary atmosphere. At the same time, the system of Eqns. (11), as noted, makes it possible to calculate the precessional motion of a gyroscopically stabilized projectile in the presence of wind. Below are the results of a number of calculations taking into account the longitudinal $W_x$ and side wind $W_z$ components on the flight trajectory at the elevation angle of $35^0$, the exit

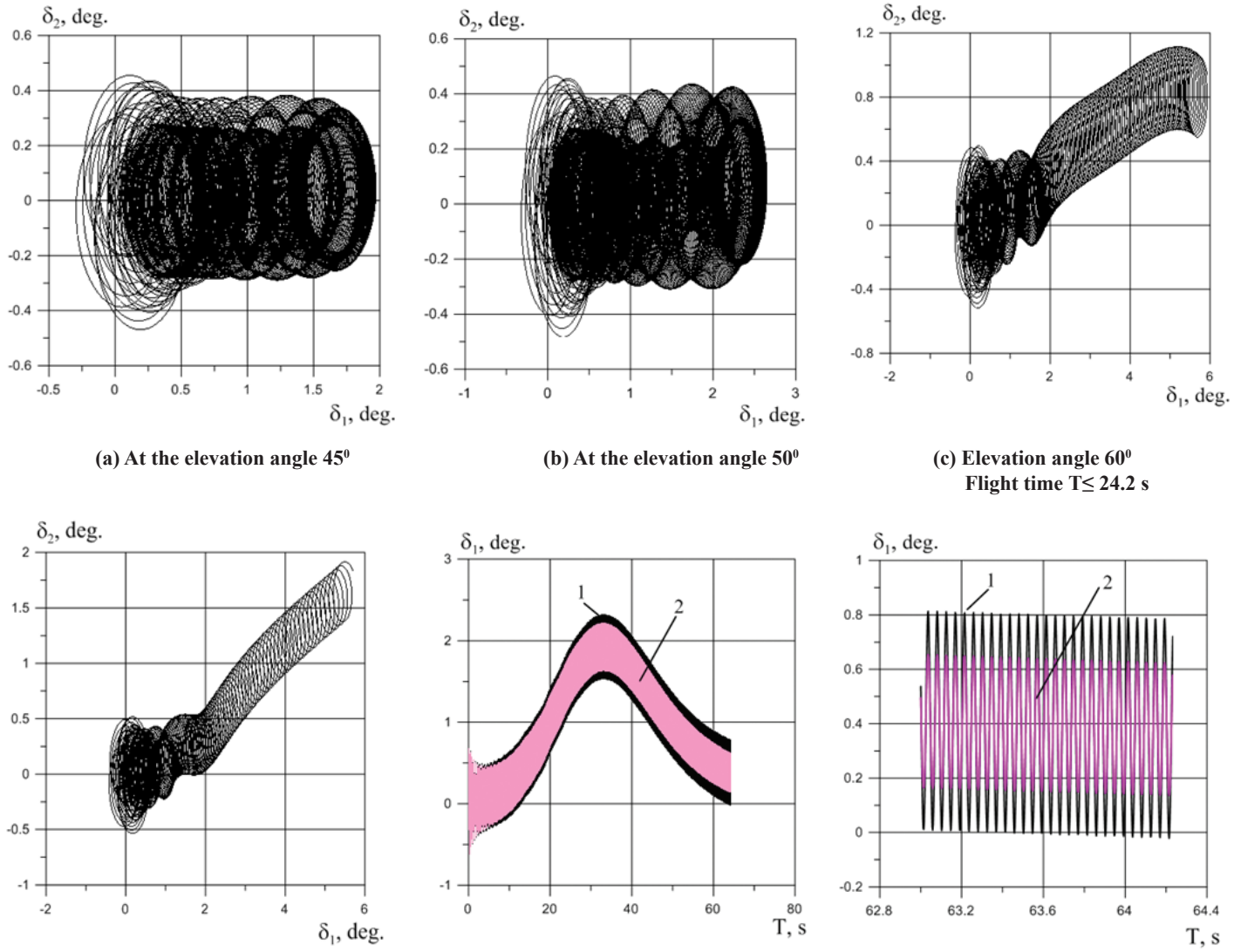


**(a) At the elevation angle $45^0$**

**(b) At the elevation angle $50^0$**

**(c) Elevation angle $60^0$ Flight time T≤ 24.2 s**

**(d) Elevation angle $65^0$ Flight time T≤ 21.9 s**

**(e) Elevation angle $70^0$ Fight time T≤ 31.93 s**

**(f) Elevation angle $70^0$ Flight time T≤ 31.09 s**

**Figure 7. Dependencies $\delta_2 = f(\delta_1)$ at the different elevation angles of the gun barrel.**

velocity $V_0$ = 930 m/s, the initial angular velocity $r_0$ = 1860 rad/s, $\delta_0 = 0.1$ deg. and $\dot{\delta}_0 = 0.15\ rad/s$ (Fig. 8). In Fig. 8(a) shows the dependence $\delta_2 = f(\delta_1)$ with a tailwind component of the longitudinal wind $W_x = 10$ m/s and $W_z = 0$. Figure 8(b) shows the dependence for the oncoming longitudinal wind component $W_x = -10$ m/s and $W_z = 0$. It can be seen that with a tailwind, the head of the projectile rises up (Fig. 8(a)). With a oncoming longitudinal wind, the head of the projectile descends by approximately the same amount (Fig. 8(b)). Dependences in Fig. 8(c) and Fig. 8(d) illustrate the calculations in the presence of a crosswind component. In Fig. 8(c) shows the dependence for the crosswind component $W_z = 10$ m/s, directed at the starting position from left to right and $W_x = 0$ in the time interval 0÷1.5 seconds. The dependence shown in Fig. 8(d) was obtained for the total flight time. In all the cases considered at the wind velocity of 10 m/s, the stability of the rotational motion was maintained throughout the entire flight trajectory. The direction of deflection of the head part of the projectile in the initial section of the trajectory is characteristic with the wind. In Fig. 8(d) it can be seen that with a left crosswind the head part deviates to the left towards the wind and somewhat downward. With a right-side wind, the head part deviates to the right towards the wind and slightly upward (Fig. 8(f)), which is consistent with the results given in [reference 5, p. 88] for a bullet fired from a rifled barrel. The analysis of the obtained dependences shows that the most dangerous is the right-side wind, which gives the greatest increase in the non-periodic component of the nutation angle and the corresponding value of the aerodynamic destabilizing moment. As before, number 1 denotes the result of the calculation without the equatorial damping moment, number 2 – with the equatorial damping moment.

### 3.6 Loss of Stability in the Crosswind

With an increase in the velocity of the right-side wind up to 20 m/s, the calculated loss of stability of the right-side rotational motion of the projectile was observed, which

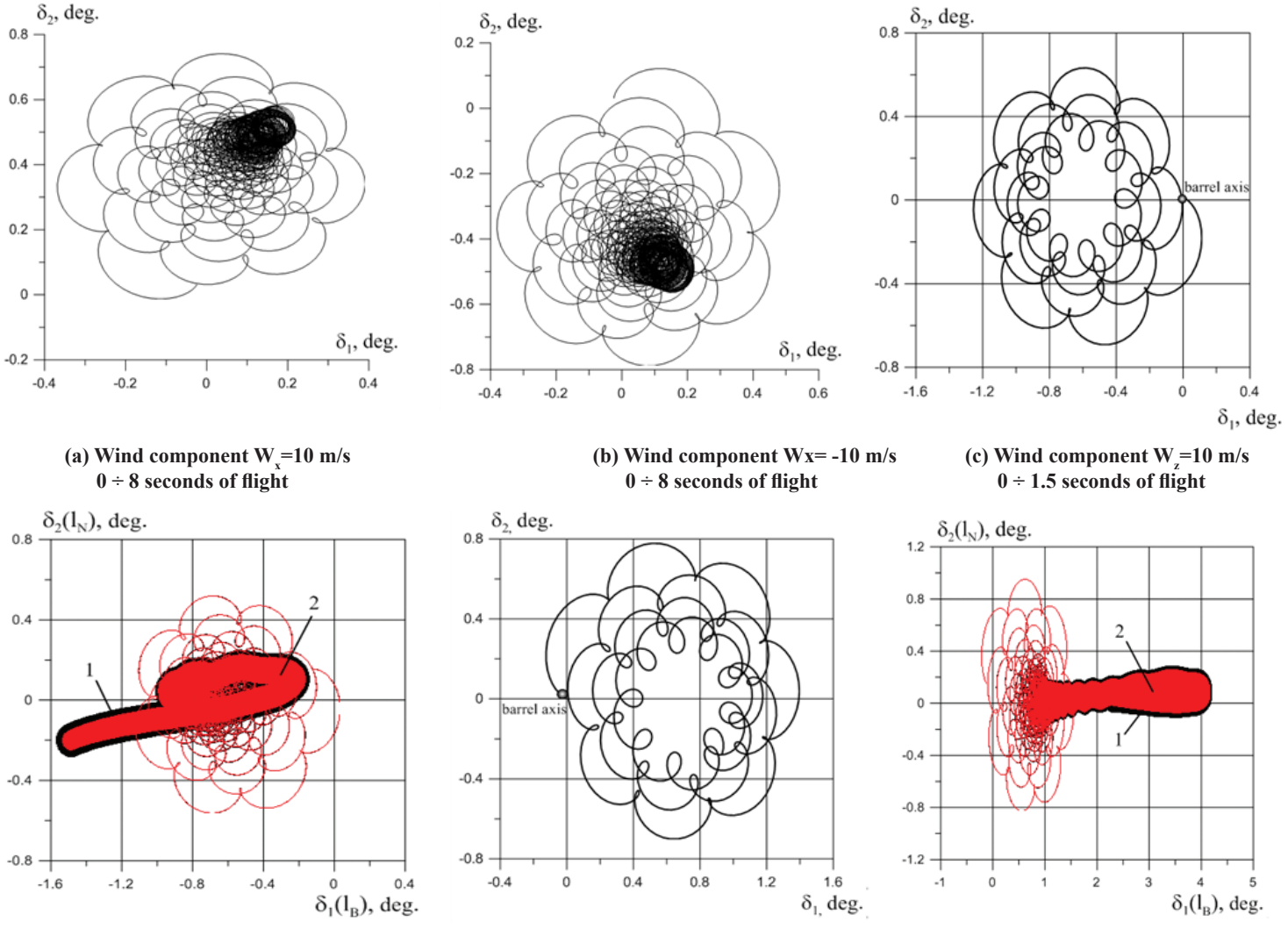


**(a) Wind component $W_x$=10 m/s 0 ÷ 8 seconds of flight**

**(b) Wind component Wx= -10 m/s 0 ÷ 8 seconds of flight**

**(c) Wind component $W_z$=10 m/s 0 ÷ 1.5 seconds of flight**

**(d) Wind component $W_z$=10 m/s Total flight time**

**(e) Right side wind $W_z$= -10 m/s 0 ÷ 1.5 seconds of flight**

**(f) Right side wind $W_z$= -10 m/s Total flight time**

**Figure 8. Dependencies $\delta_2 = f(\delta_1)$ for longitudinal $W_x$ and crosswind $W_z$.**

occurred in the immediate vicinity of the upper point of the trajectory. Fig. 9(a) and Fig. 9(b) shows the calculated loss of stability in the vicinity of the upper point of the trajectory at the right-side wind component $W_z = -20$ m/s ($W_x = 0$) at the time T=27.46 s. The estimated time to pass the top point of the trajectory is about 27.83 seconds. Fig. 9(c) shows the calculated time T dependence of the nutation angle component $\delta_1$ at a side right wind with the velocity of 20 m/s from the moment of projectile departure to the moment of loss of stability. In Fig. 9(d) shows the calculated time T dependence of the the overturning aerodynamic moment $M_S$ at the right-side wind with the velocity of 20 m/s from the moment of projectile departure to the moment of loss of stability. An increase in the non-periodic component $\delta_1$ of the angle of dynamic equilibrium to a value $\approx 6^0$ and a corresponding increase in the overturning aerodynamic moment $M_S$ to a value of the order $9.6\,N\cdot m$ at the moment of loss of stability is seen.

Shown in Fig. 9 the results of ballistic studies of the right-side rotational motion of the projectile at the righ-sidt wind velocity of 20 m/s ($W_z$ = 20 m/s) were obtained taking into account the equatorial damping moment. Ballistic calculation at the right-side wind velocity of 20 m/s ($W_z$ = -20 m/s) and the same initial conditions of the shot without taking into account the equatorial damping moment did not lead to the loss of stability of the projectile's rotational motion throughout the entire trajectory. The maximum value of the non-periodic component of the angle $\delta_1$ (the angle of dynamic equilibrium) in the calculation without taking into account the damping moment was $\delta_1 \approx 6.5^0$. In Fig. 10(a) shows together the results of this calculation (marked with 1 and in black) and dependence $\delta_1 = \delta_1(T)$ according to the calculation with damping moment, presented earlier in Fig. 9(c) (marked with 2 and in red). The further increase in the right-side wind up to 30 m/s (Wz = -30 m/s) gave similar qualitative results (Fig. 10(b)). In this case, the loss of stability in the case of calculation with a damping

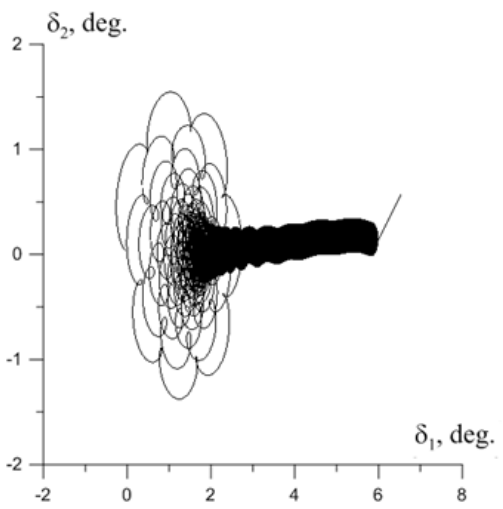


**(a) Time interval 0÷28 seconds**

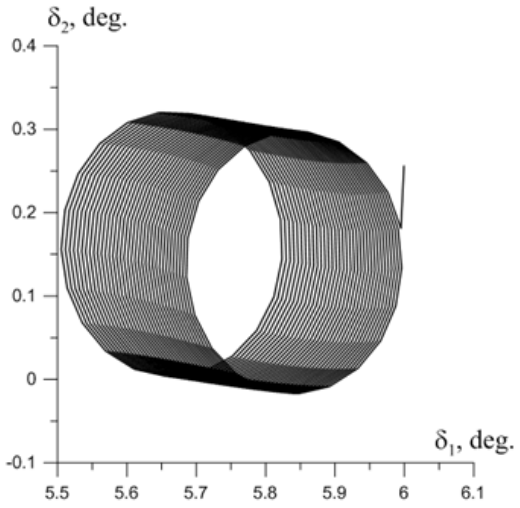


**(b) Time interval 27÷28 seconds**

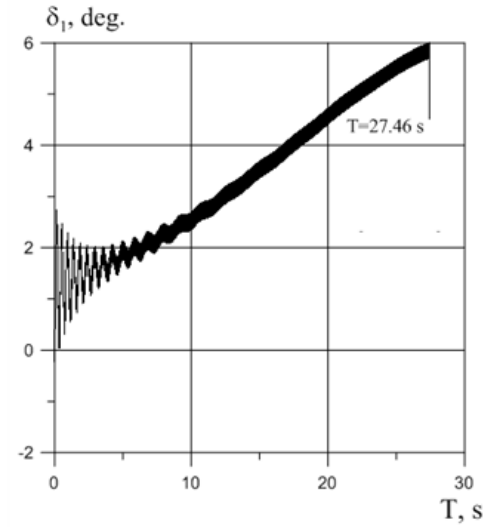


**(c) Angle component $\delta_1(T)$**

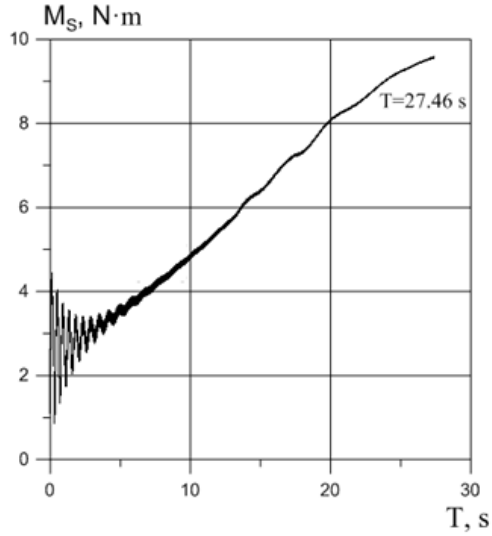


**(d) Overturning moment $M_s(T)$**

**Figure 9. The loss of stability at the right-side component of the wind WZ= -20 m/s.**

moment occurred earlier in time (T=17.24 s) in comparison with the calculation at $W_z$ = -20 m/s. The maximum value of the non-periodic component of the angle $\delta_1$ (the angle of dynamic equilibrium) in the calculation without taking into account the damping moment increased to $\delta_1 \approx 8.5^0$.

Ballistic calculations of the characteristics of the right-side rotational motion of the projectile in the left-side wind (Wz ≥20 m/s) did not show the loss of stability both without and with allowance for the equatorial damping moment. In Fig. 10(c) shows two superimposed calculated dependences of the angle $\delta_1$ on the flight time T in the left-side wind with the velocity of 20 m/s ($W_z$ = 20 m/s). It can be seen that the projectile retains its motion stability throughout the entire flight time both in the calculation without and with the equatorial damping moment. In this case, the maximum value of the non-periodic component of the angle $\delta_1$ (angle of dynamic equilibrium) in both cases is $\delta_1 \approx$-3.30. In Fig. 10(d) shows two calculated dependences of the angle $\delta_1$ on the flight time T with a left-side wind with the velocity of 30 m/s ($W_z$ = 30 m/s). It can be seen that the projectile also maintains stability of motion throughout the entire flight time both in the calculation without and with the equatorial damping moment. In this case, the maximum value of the non-periodic component of the angle $\delta_1$ increases to $\delta_1 \approx$-5.30.

Once again, let's pay attention to the fact that all previous graphic dependences, where only black color is present, were obtained when calculating taking into account the equatorial damping moment. In the case when, for comparison, two graphical dependencies are superimposed one on one, they should be distinguished as follows. Graphic dependences of red color (indicated by the number 2) were obtained during calculations taking into account the equatorial damping moment. They are superimposed on the black graphic dependences (indicated by the number 1) obtained in the calculations without taking into account the equatorial damping moment.

Presented in Figs. 9 and Fig. 10(a)-(d), the results revealed the loss of stability of the right-side rotational motion of the projectile when calculating taking into account the equatorial damping moment in the case of the presence of the right-side wind with the velocity of 20 m/s or more, in contrast to calculations without a damping moment. This result requires further careful study. The reason for the loss of stability can be called the presence of dissipative forces in the structure of acting forces. A rigorous proof that dissipative forces destroy

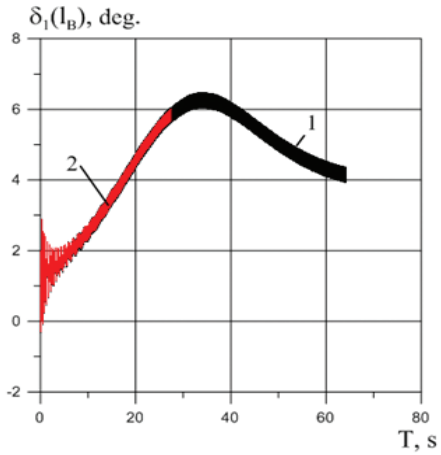


**(a) Dependences of angle $\delta_1$ from time T Right-side wind component $W_z$= -20 m/s**

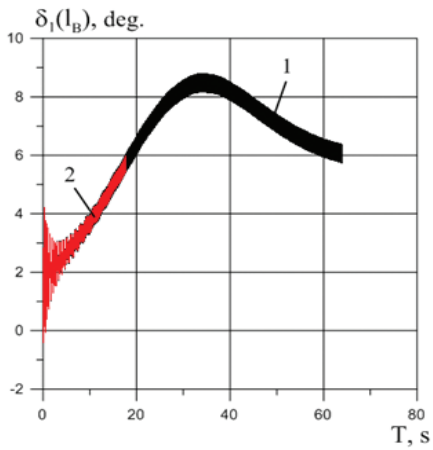


**(b) Dependences of angle $\delta_1$ from time T Right-side wind component $W_z$= -30 m/s**

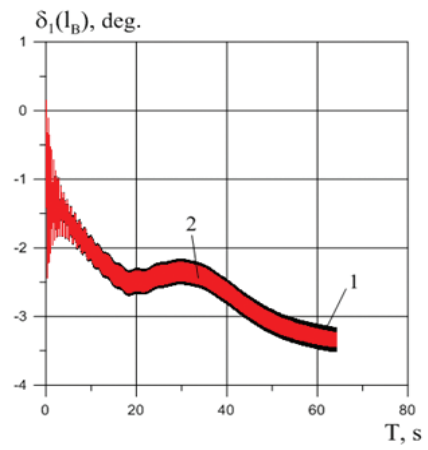


**(c) Dependences of angle $\delta_1$ from time T Left-side wind component $W_z$= 20 m/s**

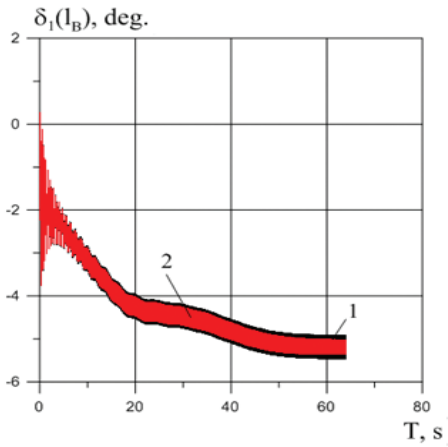


**(d) Dependences of angle $\delta_1$ from time T Left-side wind component $W_z$= 30 m/s**

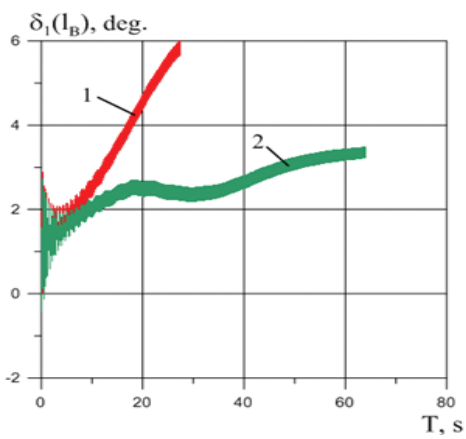


**(e) Dependences of angle $\delta_1$ from time T Right-side wind component $W_z$= -20 m/s**

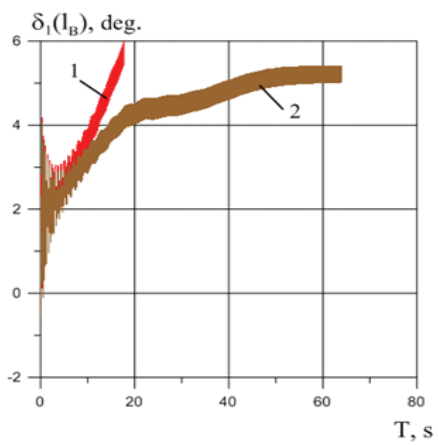


**(f) Dependences of angle $\delta_1$ from time T Right-side wind component $W_z$= -30 m/s**

**Figure 10. Results of stability calculations with and without taking into account the equatorial damping moment in the crosswind.**

the gyroscopic stabilization of an artillery shell was given by Chetaev[13], who constructed the Lyapunov function for a system of equations of the form (2).

The right-side rotational motion of the projectile, which was unstable in a right-side wind, calculated taking into account the equatorial damping moment, became stable when the direction of rotation changed to left-side. And vice versa, the unstable left-side rotational motion of the projectile with a left-side wind became stable when the wind direction changed to the right-side one. In Fig. 10(e) shows two calculated dependences $\delta_1=\delta_1(T)$. Both dependences were obtained at the elevation angle of $35^0$, the exit velocity $V_0$ = 930 m/s, the initial angular velocity $r_0$ = 1860 rad/s, $\delta_0 = 0.15$ deg., $\dot{\delta}_0 = 0.35\ rad/s$ and the right-side wind of 20 m/s ($W_z$ = -20 m/s). The dependence marked with number 1 (red) corresponds to the unstable right-hand rotation of the projectile. This buckling case was presented earlier in Fig. 9(c) and Fig. 10(a). The number 2 (brown) indicates the dependence corresponding to the stable left-side rotation of the projectile ($r_0$ = -1860 rad/s). In Fig. 10(f) shows two similar calculated dependences $\delta_1=\delta_1(T)$ with a right-side wind of 30 m/s (Wz = -30 m/s) with a change in the initial rotation velocity from $r_0$ = 1860 rad/s to $r_0$ = -1860 rad/s.

## 5. CONCLUSIONS

The method is proposed for calculating the equatorial damping moment of an axisymmetric rotation bodies such as the artillery projectile in the counter flow on the flight trajectory. The method has been tested in ballistic studies of the rotational motion of the artillery projectile. The method is based on differentiation of the dependence of the overturning aerodynamic moment by the angle of attack and the Mach number of the oncoming flow. This dependence can be obtained by numerical simulation using modern software systems, existing calculation-experimental dependences or the results of special experiments. In this paper, the values of the aerodynamic overturning moment at given Mach numbers and angles of attack of the oncoming flow were determined by numerical simulation. The tabulated dependence of the aerodynamic overturning moment was differentiated on the calculated flight trajectory at the calculated Mach numbers and angles of attack. Based on the known criterion of dynamic stability using the proposed method for calculating the equatorial damping moment, a ballistic analysis of the rotational motion of a gyroscopically stabilized artillery projectile on the flight trajectory was carried out, which confirmed its asymptotic instability. Based on the known equations of motion, which take into account the action of the equatorial damping moment, ballistic studies of the parameters of the perturbed rotational motion of the 155-mm artillery projectile were carried out. A significant effect of the equatorial damping moment on the magnitude of the periodic components of the projectile precessional motion and the absence of the noticeable effect on their non-periodic components in comparison with calculations without taking into account the equatorial damping moment are shown. The given calculation examples of the loss of stability of the rotational motion of the projectile in the initial section of the trajectory as the result of the decrease in the initial projectile rotation velocity and at large angles of shot showed that the values of the parameters of the rotational motion of the projectile, which are boundary in terms of stability, obtained using the equatorial damping moment, do not noticeably differ from the values in the calculations without the equatorial damping moment. At the same time, the results of ballistic calculations with the loss of stability of the rotational motion of the projectile in the presence of the side wind showed the destabilizing effect of the equatorial damping moment in the case of the projectile spinning towards the side wind. The independent criterion for assessing the stability of rotating projectiles on the curved section of the trajectory can be the angle of dynamic equilibrium, which in all calculated examples showed the automodel properties with respect to the equatorial damping moment.

## REFERENCES


1. McCoy, R.L. *Mod. Exter. Ballistics.* Schiffer Publishing, Ltd., 2004, 328. https://www.abebooks.com/book-search/title/modern-exterior-ballistics/author/robert-mccoy/
2. Carlucci, D.E. & Jacobson, S.S. *Ballistics, Theory and Des. of Guns and Ammunitions*. CRC Press. Taylor & Francis Group, 2014, 586 pp. https://www.taylorfrancis.com/books/mono/10.1201/b15495/ballistics-donald-carlucci-donald-carlucci-sidney-jacobson
3. Klimi, G. *Exter. Ballistics: A New Approach.* Xlibris. 2010, 402 pp. https://books.google.com/books/about/Exterior_Ballistics.html?id=UbuB4Erc3CEC
4. Dmitrievskij, A.A. *Exter. Ballistics.* Moscow: Mashinostroenie, 2005, 608 pp. (in Russian). https://www.studentlibrary.ru/kk/book/ISBN5217032529.html
5. Litz, B. *Appl. Ballistics for Long-Range Shooting. Third Edition*. Applied Ballistics LLC, 2015, 432 pp. https://www.pdfdrive.com/applied-ballistics-for-long-range-shooting-e6227289.html
6. Baranowski, L. Numerikal testing of flight stability of spin-stabilized artillery projectiles. *J. Theor. Appl. Mech.,* 2013, **51**(2), 375-385. https://www.researchgate.net/publication/290771580_Numerical_testing_of_flight_stability_of_spin-stabilized_artillery_projectiles
7. Khalil, M.; Abdalla, H. & Osama, Kamal. Dispersion Analysis for Spinning Artillery Projectile. *13th Int. Conf. ASAT-13,* Cairo, Egypt, 2009, Military Technical College, Cairo, Egypt, Paper: ASAT-13-FM-03, 2008, 1-12. doi: 10.13140/RG.2.1.4538.1844
8. Thuresson, M. Development and evaluation of a six degrees of freedom model of a 155 mm artillery projectile. *Master of Sci. Thesis MMK 2015:94 MDA 523,* KTH Royal Institute of Technology, Industrial Engineering and Management. Stockholm, Sweden, 2015, 1-40 (PhD Thesis). http://www.diva-portal.org/smash/get/diva2:905698/FULLTEXT01.pdf

9. Krylov, A.N. *Collect. of works. T.IV, Ballistics*. Moscow: Academy of Sciences of the USSR, 1937, 444. (in Russian).
http://www.math.ru/lib/files/pdf/krylov/ANK-04.pdf
10. Awad, I. Saleh; Mohamed, M.M.; Hasan, Noha; M.M. Darwish. The Mikhailov Stability Criterion Revisited. *J. Eng. Sci., Assiut University*, 2010, **38**(1), 195-207.
doi: 10.21608/JESAUN.2010.123808
11. Newill, J.F.; Guidos, B.J. & Livecchia, C.D. 2003. Validation of the U.S. Army Research Laboratory's Gun Dynamics Simulation Codes for Prototype Kinetic Energy. U.S. Army Research, Development and Engineering Center, *ARL-TR-3039*, 2003, 1-21.
https://ia800105.us.archive.org/12/items/DTIC_ADA418039/DTIC_ADA418039_text.pdf
12. Garner, J.M.; Guidos, B.J.; Soencksen, K.P. & Webb, D.W. Flat Fire Jump Performance of a 155-mm Ml98 Howitzer. Weapons and Materials Research Directorate, Army Research Laboratory, Aberdeen Proving Ground, *ARL-TR-2067*, 1999, 1-41.
https://apps.dtic.mil/sti/pdfs/ADA369710.pdf
13. Chetaev, N.G. On the stability of rotational motions of projectiles. *Appl. Mathematics and Mech.*, 1946, **10**(1), 135-138.
http://ikfia.ysn.ru/wp-content/uploads/2018/01/Chetaev1965ru.pdf

## CONTRIBUTORS

**Dr Oleksandr M. Shyiko** is graduate from the National Aerospace University (formerly "Kharkiv Aviation Institute"), Kharkiv, Ukraine. He obtained a PhD in Technical Sciences from the National Technical University "Kharkiv Polytechnic Institute", Kharkiv, Ukraine, specializing in Dynamics and Strength of Machines. He worked as an Associate Professor at the Sumy State University and until recently at the Sumy National Agrarian University. He also worked as a Senior/Leading Researcherat the Research Center of the Missile Forces and Artillery, Sumy, Ukraine, focusing on research in applied aerodynamics and ballistics. His areas of research interest include: Vibrations of machines, aerodynamics, external ballistics.
His contribution to this research–Development of computational models, algorithm and computational program, calculations, analysis of the obtained data, data visualization, textwriting and editing.

**Dr Olexii A. Obukhov** holds PhD in Technical Sciences, and is Associate Professor. He holds a PhD from the Odessa National Academy of Food Technologies, Odessa, Ukraine, specializing in refrigeration, vacuum and compressor engineering, and air conditioning systems. He held a position of a researcher at the Research Center of the Missile Forces and Artillery, Sumy, Ukraine.Currently, he is an Associate Professor with the Department of Physics at the Sumy National Agrarian University. His areas of research interest include: Aerodynamics, heat transfer, external ballistics. He resides in Sumy, Ukraine.
His contribution to current research–computational modeling of aerodynamic longitudinal force, aerodynamic shear force and aerodynamic overturning moment coefficients.